Extensive Air Showers, Lightning, and Thunderstorm Ground Enhancements

Article *in* Astroparticle Physics · May 2016

DOI: 10.1016/j.astropartphys.2016.04.006

3 authors, including:

Ashot Chilingarian
Yerevan Physics Institute
372 PUBLICATIONS **4,680** CITATIONS

SEE PROFILE

Astroparticle Physics 82 (2016) 21–35

Contents lists available at ScienceDirect

Astroparticle Physics

journal homepage: www.elsevier.com/locate/astropartphys

Extensive air showers, lightning, and thunderstorm ground enhancements

A. Chilingarian[a,b,*], G. Hovsepyan[a], L. Kozliner[a]

[a] A. Alikhanyan National Lab (Yerevan Physics Institute), 2 Alikhanyan Brothers, Yerevan 0036, Armenia
[b] National Research Nuclear University MEPhI (Moscow Engineering Physics Institute), Moscow 115409, Russian Federation

ARTICLE INFO

Article history:
Received 1 October 2015
Revised 12 March 2016
Accepted 30 April 2016
Available online 16 May 2016

Keywords:
Lightning
Atmospheric electricity
Thunderstorm ground enhancements
Extensive air showers

ABSTRACT

For lightning research, we monitor particle fluxes from thunderclouds, the so-called thunderstorm ground enhancements (TGEs) initiated by runaway electrons, and extensive air showers (EASs) originating from high-energy protons or fully stripped nuclei that enter the Earth's atmosphere. We also monitor the near-surface electric field and atmospheric discharges using a network of electric field mills.

The Aragats "electron accelerator" produced several TGEs and lightning events in the spring of 2015. Using 1-s time series, we investigated the relationship between lightning and particle fluxes. Lightning flashes often terminated the particle flux; in particular, during some TGEs, lightning events would terminate the particle flux thrice after successive recovery. It was postulated that a lightning terminates a particle flux mostly in the beginning of a TGE or in its decay phase; however, we observed two events (19 October 2013 and 20 April 2015) when the huge particle flux was terminated just at the peak of its development. We discuss the possibility of a huge EAS facilitating lightning leader to find its path to the ground.

1. Introduction

Considered the highest peak in the South Caucasus, Mount Aragats is a dormant volcano with a 400-m deep crater that has become an ice basin. Its central highlands cover an area of $> 820\,km^2$ and generate huge summer storms that flow down its slopes into the surrounding valleys. The four crests that top Mt Aragats once reached heights $> 10{,}000$ m 1.5 million years ago, before a massive eruption lowered them to its current 4095 m. Only in 100 km to the south of Mt Aragats across the valley of the Araks River stands the sister of Aragats – Biblical Mount Ararat. Lightning events are pronounced at Aragats; thus, it is considered the home of the ancient Armenian god of thunder and lightning, Vahagn. Mt Aragats houses one of the world's oldest and largest cosmic ray (CR) research stations, located on its slopes. The Cosmic Ray Division (CRD) of the A. Alikhanyan National Laboratory (Yerevan Physics Institute) during the last 70 years has commissioned and operated on the research stations of Aragats and Nor Amberd numerous particle detectors uninterruptedly registers fluxes of charged and neutral CRs. The research work at Aragats (in the framework of Aragats Space Environment Center (ASEC, [5]) includes registration of extensive air showers (EAS) with large particle detector arrays, investigation of solar–terrestrial connections, monitoring of space weather, and observation of high-energy particles from the thunderclouds. More than 300 particle detectors (including plastic scintillators and NaI spectrometers) register particle fluxes and send data online to the CRD headquarters in Yerevan. In addition to particle detectors, ASEC includes facilities that can measure electric and geomagnetic fields, lightning strenth and locations, and a variety of meteorological parameters. With the installation of fast electric field recorders and automotive cameras in 2014, research on lightning physics started on Aragats. ASEC facilities are located on the slopes of Mt Aragats and in Yerevan at altitudes of 3200, 2000, and 1000 m above sea level (Fig. 1). The distance between Nor Amberd and Aragats research stations is 12.8 km. The CRD headquarters is located at distances of 26.5 and 39.1 km from the Nor Amberd and Aragats research stations, respectively. The geographical coordinates of the Nor Amberd station, Aragats station, and Yerevan Physics Institute are 40.3750°N, 44.2640°E; 40.4713°N, 44.1819 E; and 40.2067 N, 44.4857 E, respectively.

Acceleration and multiplication of CR electrons by the strong electric fields in the thunderclouds are well-established phenomena constituting the core of the atmospheric high-energy physics; they are related to runaway breakdown [18], recently referred to as relativistic runaway electron avalanches (RREAs, [15,16]). However,

* Corresponding author at: A. Alikhanyan National Lab (Yerevan Physics Institute), 2 Alikhanyan Brothers, Yerevan 0036, Armenia. Tel.: +37410352041.
E-mail address: chili@aragats.am (A. Chilingarian).

http://dx.doi.org/10.1016/j.astropartphys.2016.04.006
0927-6505/

Fig. 1. Snapshot of Google map of Mt Aragats with Aragats and Nor Amberd research stations and Yerevan headquarters of CRD.

the origin and location of charged centers in the thundercloud (one of the most important aspects in the atmospheric physics) have not been clear until now. In fair weather conditions, the atmosphere is positively charged and the Earth has an opposite-polarity negative charge. A thunderstorm can drastically change the pattern of cloud electrification. A simple sketch of storm-time cloud electrification is shown in Fig. 2. The top layer of the thundercloud has a positive charge with a negative screening layer just above it; the middle layer has a negative charge and a small local region of positive charge is present the bottom of the cloud [25]. If we use the so-called "physics" sign convention (see discussion on the used sign conventions by Krehbeil et al. [21]), then the near-surface electrostatic field is negative during fair weather (positive ions slowly migrate from the atmosphere toward the Earth) and positive during thunderstorms (electrons are transported by the lightning from the cloud to the Earth). According to the tripole model (quadruple, if we add a negative screening layer above the main positive layer), there exist several dipoles of opposite orientation in the cloud, which accelerate electrons downward, in the direction of the Earth and toward open space, as shown in Fig. 2. The "atmospheric electricity" sign convention shows the opposite trend: the fair-weather near-surface electric field is positive and the storm-time field is mainly negative. The historical basis of this controversy is that the electric mills usually operated according to the "atmospheric electricity" sign convention (positive and negative electric fields at the ground are produced by positive and negative charge overheads, respectively). Thus, a recorded positive field change corresponds to a negative lightning, which decreases the negative charge overhead, and negative field change corresponds to a positive lightning, which decreases the positive charge overhead. Our key evidence for lightning research is the monitoring of particle fluxes from thunderclouds. These fluxes significantly increase the usually stable background of the secondary CRs incident on the Earth's surface and create the so-called thunderstorm ground enhancements (TGEs, [6,7]). Development of a lower positive charge region (LPCR) facilitates the proper direction of the electric field, in order to accelerate the electrons in the direction of the Earth. The upper dipole accelerates electrons upward and radiated bremsstrahlung gamma rays reaching the satellites are registered by the orbiting gamma-ray observatories. These enigmatic bursts of gamma rays are termed as terrestrial gamma-ray flashes (TGFs, [17]). The particle burst in the gap between the positive upper layer and the screening layer recently detected by ADELE aircraft [20] is named gamma flow.

Both the lightning initiation and leader propagation and the dynamics of TGE are dependent on the cloud electrification and, therefore, on the charged layers in the thundercloud. Thus, by detecting the changing particle fluxes, we can monitor the distribution of charged layers above the particle detector site. As the nearest to the ground charged layer, LPCR strongly affected the development of cloud-to-ground (CG) and intracloud (IC) discharges and TGEs. When LPCR is above the particle detectors, and when the field is sufficiently strong, the electric field between LPCR and the main negatively charged region above effectively accelerate

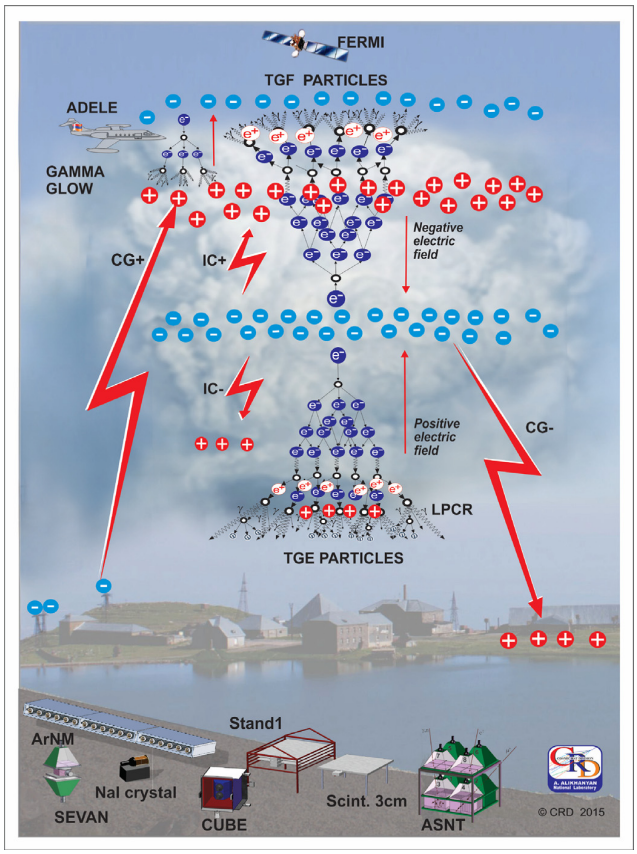

Fig. 2. High-energy physics processes in the atmosphere.

electrons downward [9]. Thus, the intensity and energy spectra of gamma rays and electrons of TGE can be used for estimating the position and thickness of the LPCR.

At the maximum of the TGE flux, in the time series of the near-surface electric field, we usually observe the so-called "bumps" rising from deep negative electric field – a small increase of the electric field with amplitude up to 10–20 kV/m. It was postulated [22] that particularly in the declining phase of the TGE, negative CG lightnings often occur, which abruptly terminates the particle flux [1,11,24]. The mature LPCR does not allow a lightning leader to reach the ground, declining it horizontally and transforming a CG lightning attempt to an IC lightning. A CG lightning becomes energetically more preferable than an IC one when LPCR is thin. However, sometimes a catastrophic decay of TGE can be seen near the maximum of the particle flux. High-energy EASs (with primary particle energies $>10^{16}$ eV) possibly facilitated the propagation of the lightning leader downward [19]. Therefore, we discuss a large EAS registration by the Aragats neutron monitor and muon detectors during thunderstorms.

Characteristic patterns of the electrostatic field disturbances make it possible to determine the polarity of the lightning: an increase in the field strength (within 0.1–1 s) with consequent slow recovery (10–30 s) corresponds to negative lightning, whereas a decrease of field strength corresponds to positive lightning. The electric mill network at the slopes of Mt Aragats also allows distinguishing between CG and IC lightning events [14]. If no electrostatic field reversal occurred, we classify the lightning as a CG one, and at any reversal occurrence – an IC one [21]. It is worth noting that all the TGE-terminating lightning events are of the CG type.

The absolute value of the amplitude of the field change can reach and exceed 50 kV/m. Detection of lightning sometimes is confirmed by the simultaneous detection with World Wide Lightning Location Network (WWLLN; http://wwlln.net/) and photographs of the sky with lightning images. However, WWLLN registered only the strongest lightnings and the daytime and distant lightning events usually escape recording. Therefore, investigation of the relationship between lightning and TGE can explore the long-standing problem of the physical model of lightning initiation. The fundamental origin of lightning is indeed not thoroughly understood. The Aragats "electron accelerator" produced several TGE events accompanied by lightning detection in the spring of 2015. In this study, we analyze these events for deeper insights into the physics of lightning and TGE.

2. Instrumentation

The ASEC particle detectors can measure the fluxes of the species of secondary CRs (electrons, gamma rays, muons, and neutrons) as well as the electron, muon, and neutron content of EASs. Numerous thunderstorm-correlated events, detected by the ASEC facilities, constitute a rich experimental set for the investigation of the high-energy phenomena in the thunderstorm atmosphere. The new generation of ASEC detectors consists of 1- and 3-cm-thick molded plastic scintillators arranged in stacks and cubic structures. The "STAND1" detector comprised three layers of 1-cm-thick, 1-m^2 sensitive area molded plastic scintillators fabricated by High Energy Physics Institute, Serpukhov, Russian Federation. Light from the scintillator through optical spectrum-shifter fibers is reradiated to the long-wavelength region and passed to the photomultiplier FEU-115 M. The maximum of luminescence is emitted at the 420-nm-wavelength region, with a luminescence time of approximately 2.3 ns (for details of detector setup, see [12]).

The Aragats neutron monitor (ArNM, Fig. 3) consists of 18 cylindrical proportional counters of CHM-15 type (length 200 cm, diameter 15 cm) filled with BF_3 gas enriched with B^{10} isotope and grouped into three sections containing six tubes each. The proportional chambers are surrounded by 5 cm of lead (producer) and 2 cm of polyethylene (moderator). The cross section of lead producer above each section has a surface area of 6 m^2, and the total surface area of three sections is 18 m^2. The atmospheric hadrons produce secondary neutrons in nuclear reactions in lead. Then, the neutrons were thermalized in a moderator, enter the sensitive volume of the counter, and yield Li^7 and α particle via interactions with boron gas. The α particle accelerates in the high electrical field inside the chamber and produces a pulse registered by the data acquisition electronics. The high-energy hadrons generate a large number of secondary neutrons entering the sensitive volume of the proportional counter, and if all pulses initiated by the incident hadrons need to be counted, the dead time of the NM should be maintained very low (the ArNM has a minimal dead time of 0.4 μs). If only the incident hadrons need to be counted (a one-to-one relationship between count rate and hadron flux), the dead time must be as long as the whole secondary neutron collection time (~1250 μs), to avoid double-counting.

Stenkin et al. [23] described detection of the so-called neutron bursts in the NM related to occasional hitting of it by a core of high-energy EAS. More EAS hadrons will generate numerous thermal neutrons and enormously increase the NM count rate (size of the neutron burst or peak multiplicity). This option of EAS core detection by NM was almost not recognized, because the long dead time does not allow counting of all secondary neutrons. With establishing short dead time and collecting time for ArNM (usually only 1-min time series are available for NM), we detect numerous EASs hitting NM, several of which provide multiplicities above 1000. In our terminology, the multiplicity is the number of pulses

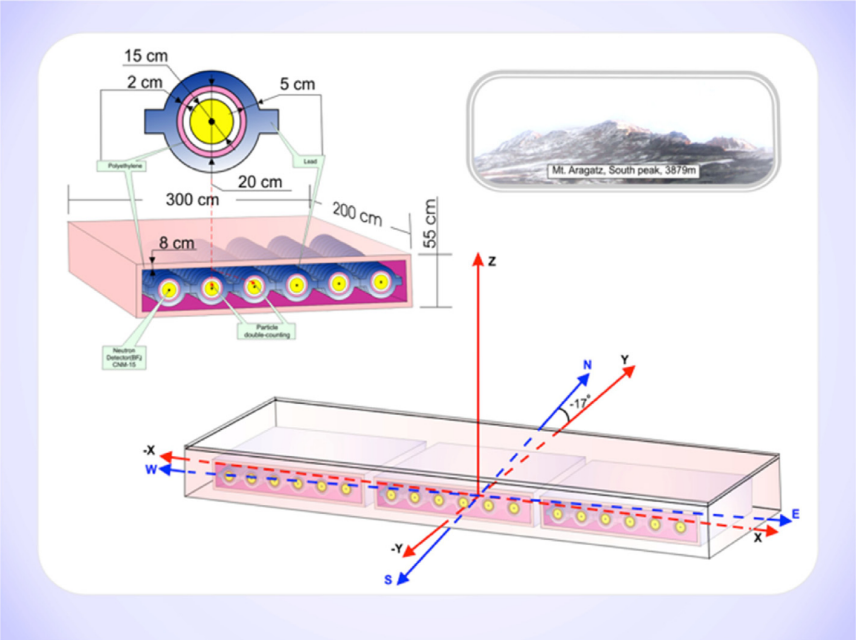

Fig. 3. Layout of Aragats Neutron Monitor (ArNM).

registered in each particular second. Each counter has a mean multiplicity of 30–60 counts per second; at a neutron burst, the multiplicity can reach several hundreds and even thousands. For each channel, we also calculate the number of standard deviations (N of σ) of the peak multiplicity. The 1-s time series of ArNM counts are being entered in the MSQL database at CRD headquarters (available at http://adei.crd.yerphi.am/adei/) as well as in the database of the Euro-Asian consortium of neutron monitors (NMDB@.eu.org).

The Aragats muon detector (Fig. 4) consists of three vertically stacked plastic scintillators with an area of 1 m^2. The top 3-cm-thick scintillator is covered by 7.5 cm of lead filter; the middle 1-cm-thick scintillator is covered by 1.5 cm of lead filter and an approximately 60-cm-thick rubber layer (carbon); and the bottom 1-cm-thick scintillator is covered by a 6-cm-thick lead filter. The energy thresholds to detect muons in three stacked scintillators are approximately 170, 220, and 350 MeV. DAQ electronics provides 50-ms time series of all scintillators.

ArNM and muon detectors are located at a distance of approximately 6 m in the MAKET experimental hall (Fig. 5). Close location of these detectors allows joint detection of several large EASs. The STAND1 detector located outdoor comprised three layers of 1-cm-thick, 1-m^2-area molded plastic scintillators and 3-cm-thick plastic scintillator of the same type. On the roof of MAKET building are located meteorological devices measuring the near-surface electric field and weather conditions. A deep negative near-surface electric field is a necessary condition for TGE origination. Moreover, the observed changes in the electric field as well as detected particle fluxes contain information on the dynamics of the cloud electrification; such information is very difficult to acquire by in situ measurements. Electrical mill EFM 100 produced by Boltek operates with a frequency of 20 Hz performing 20 measurements of the near-surface electric field per second. Professional Davis Instruments Vantage Pro2 (http://www.davisnet.com) provides a wide range of meteorological parameters measured each minute. Devices of the same type are located at the Nor Amberd research station and in Yerevan.

An array of plastic scintillators located inside and outside the MAKET hall (green "pyramids" in Fig. 5) is a part of the MAKET-ANI

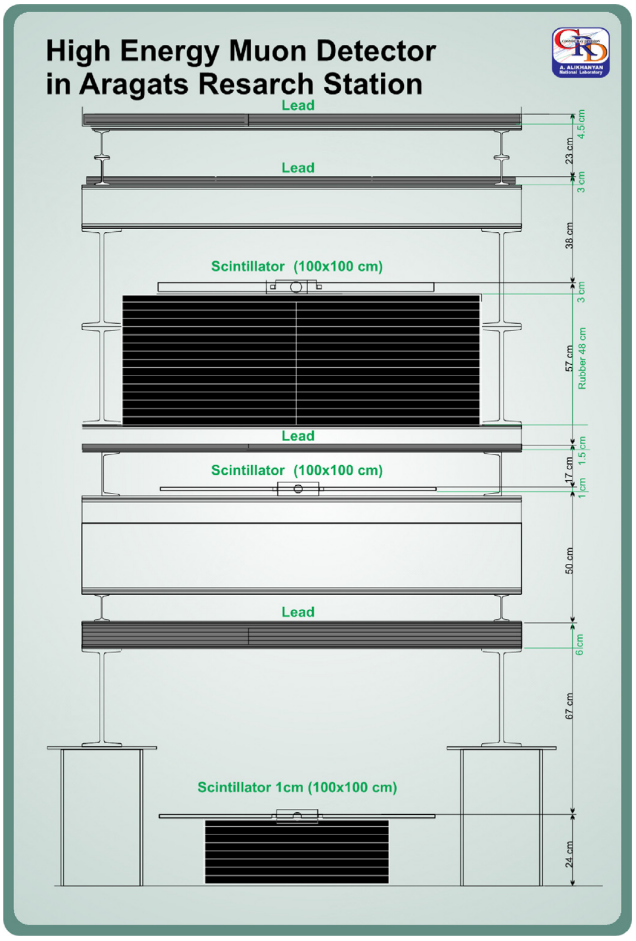

Fig. 4. "Muon" stacked detector with large amount of lead and rubber between three scintillators.

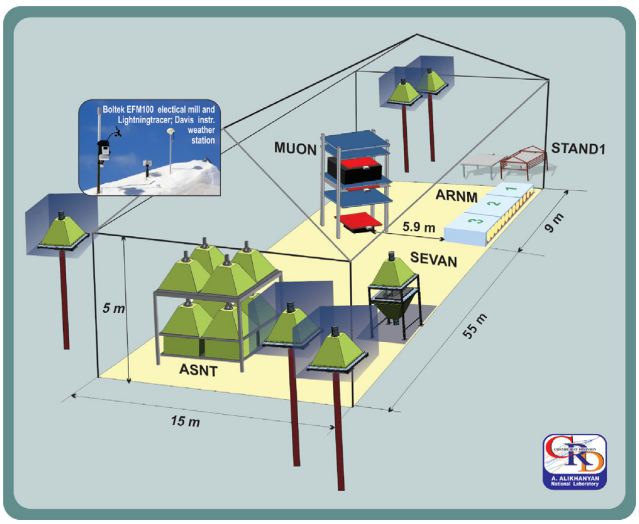

Fig. 5. MAKET experimental hall and extensive air shower (EAS) array.

experiment (Chilingarian et al. [4]. Approximately 100 detecting channels produced from 5-cm-thick plastic scintillators with an area of 1 m^2 each were triggered by large EASs corresponding to primary particle with energy $>10^{14}$ eV. At the end of the MAKET-ANI experiment, we picked several detectors and implemented special trigger conditions to detect large particle bursts due to thunderstorm activity. The MAKET detectors measure the charged species of secondary CRs with very high accuracy. Each of the stand-alone scintillators can measure incident particle flux, and the array, as a whole, can count the so-called EAS triggers ("firing" of more than eight detectors of the array within a time window of 400 ns). If the signals from the first eight scintillators coincide within the trigger window time, then the amplitudes of all photomultiplier signals (proportional to the number of particles hitting each scintillator) are stored. In fair weather, the surface array registered EASs initiated by the primary protons with energies >50 TeV (~25 EASs per minute, eightfold coincidences) and 100 TeV (~8 EASs per minute, 16-fold coincidences).

Large TGEs can trigger the MAKET array. When thunderstorm clouds are very low above the scintillators, the TGE electrons reach the MAKET scintillators and the stable EAS count rate suddenly increases. We investigate in detail these extensive cloud showers (ECSs) and prove their systematic difference from EASs [7]. ECSs are individual RREA cascades from a single CR electron entering the RREA process. Alex Gurevich et al. [19] called this cascades micro-runaway breakdown (MRB). Registration of ECSs is very difficult due to fast attenuation of electrons in the atmosphere; only at Aragats, due to very low thunderclouds, can we register several huge TGEs accompanied by ECSs [10]. ECSs are an analog of TGFs registered by orbiting gamma-ray observatories; however, TGF particles are mostly gamma rays, not electrons. Gamma rays can travel hundreds of kilometers in the open space and occasionally hit fast-moving satellites and produce very short bursts of radiation.

3. TGEs detected in spring 2015

The first spring storm started at Aragats on March 30 11:15 UT and continued until 11:50 UT with numerous nearby lightning events (Fig. 6). Thick clouds covered the sky, reducing the solar radiation by a factor of 2.5, from 370 W/m^2 at 11:32 UT down to 150 W/m^2 at 11:43 UT. The relative humidity was very high (96%). Numerous lightning events caused frequent near-surface electric field disturbances. Because of a nearby lightning (2 km far from the detector site, measured by EFM-100 electric mill), the near-surface electric field changed from −21 to +38 kV/m in <1 s (Fig. 6). The lightning terminated the particle flux registered by the STAND1 detector. For 3 s (from 11:46:59 to 11:47:01 UT), the particle count rate of the 1-m^2 scintillator correspondingly increased by 9.2%, 12.2%, and 16% above the mean value measured just before the start of the particle flux enhancement. At 11:47:02 UT, the particle flux was abruptly terminated and dropped by approximately 17%.

On April 4, the 3-cm-thick plastic scintillators detected a large TGE at 16:01 UT. In Fig. 7, instead of particle detector count rates, the corresponding *p*-values of statistical test are shown. The significance of the detected peaks in the time series of the particle count rates is determined by the actual peak values divided by the standard deviation of the count rate, that is, by the number of standard

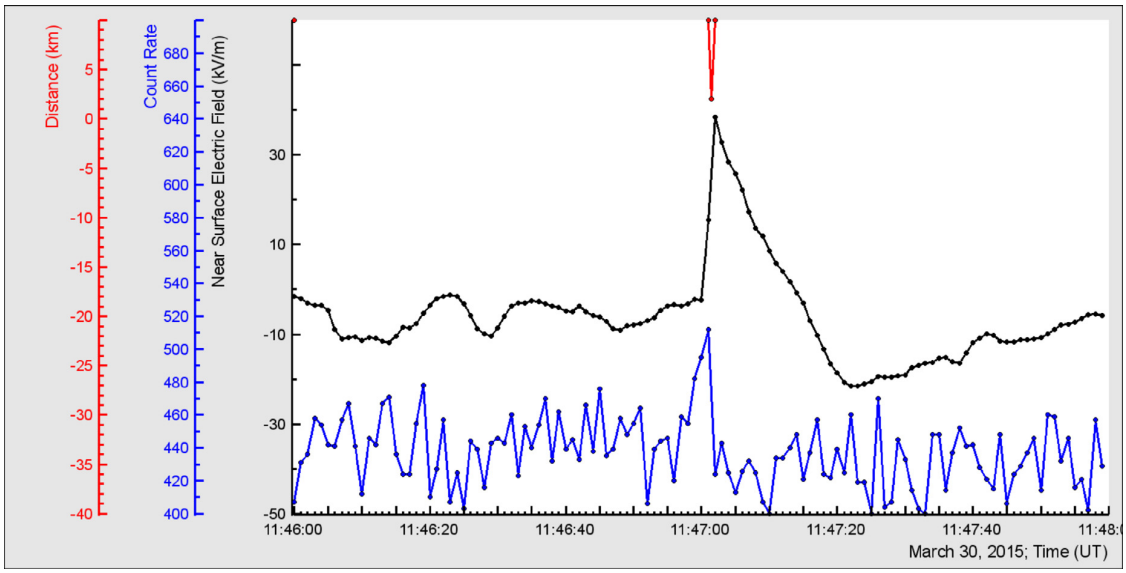

Fig. 6. One-second time series of the count rates measured by the outdoor 3-cm-thick, 1-m^2-area scintillator (bottom); 1-s time series of the near-surface electric field (middle); and distance to lightning (top).

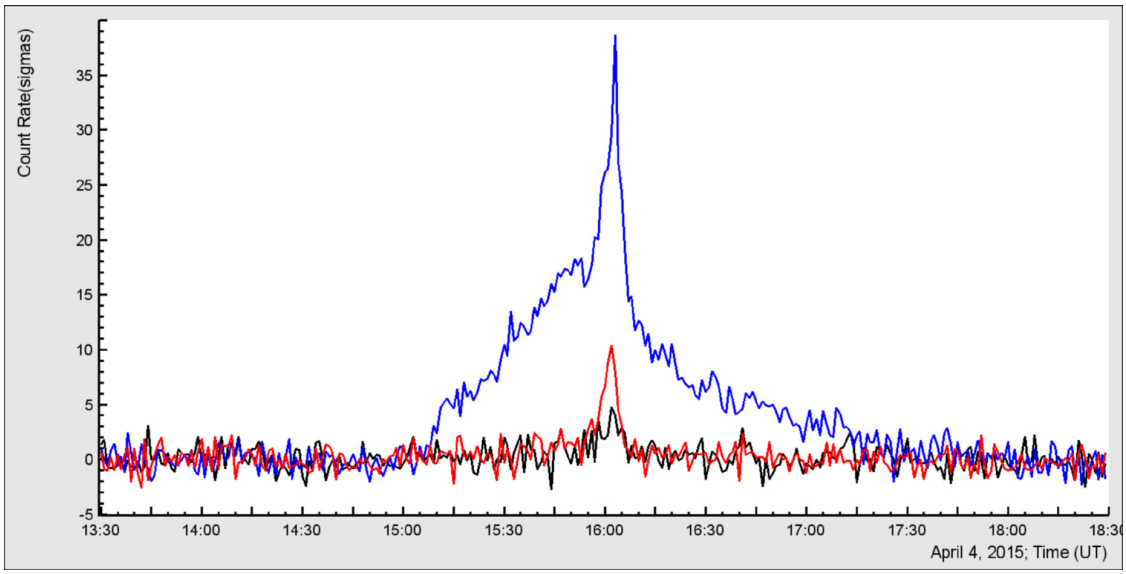

Fig. 7. Significance of the particle flux enhancements in number of standard deviations ($N\sigma$); the outdoor 3-cm-thick scintillator (free of snow) shows a 2-h TGE with a maximum of 38 σ (upper curve); the same type of indoor scintillator shows only a few-minute TGE with a maximum of approximately 10 σ enhancement (the second highest peak) and a same type of scintillator under deep snow shows only 5 σ enhancement (the smallest peak).

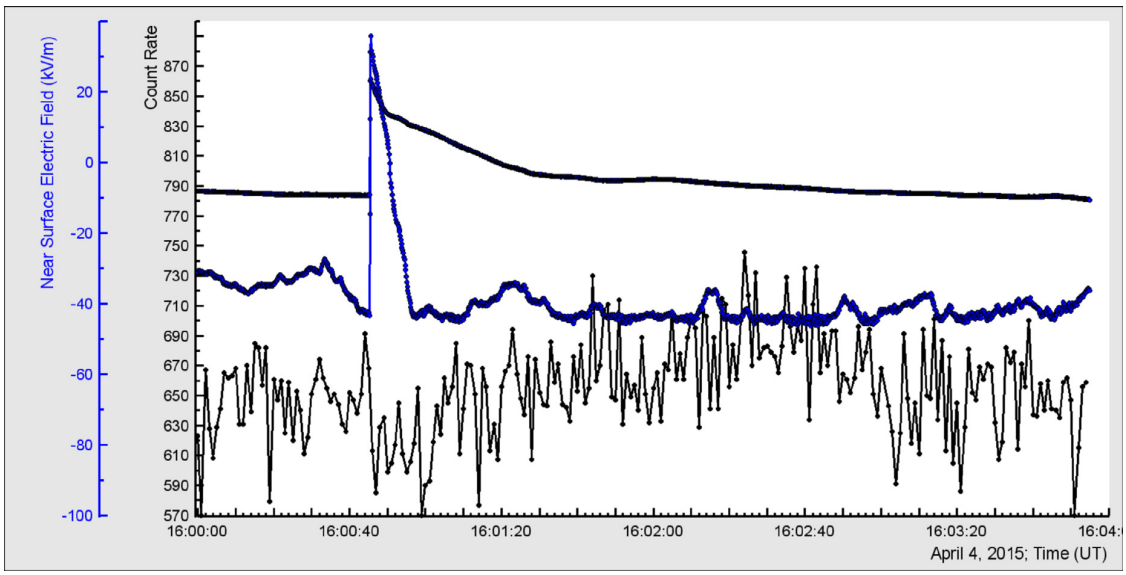

Fig. 8. One-second time series of the count rates measured by the outdoor 3-cm-thick, 1-m^2-area scintillator (bottom); near-surface electric field (middle, with larger amplitude – Aragats; top, with lower amplitude – Nor Amberd; Particle flux measured at Aragats declined by 12% after lightning at 16:00:47 UT.

deviation contained in the peak (number of σ). The p value is the most comprehensive measure of the reliability of detecting peaks in a time series. A large p value corresponds to a small probability that the observed peak is a background fluctuation and not a genuine signal. Therefore, we can safely reject the null hypothesis (that peak is a background fluctuation only) and confirm the existence of a TGE. The outdoor 3-cm-thick scintillator measures 38 σ enhancement; the same type of scintillator located indoors at another experimental hall (named SKL) shows approximately 10 σ enhancement; the scintillator located under deep snow (snow covers Aragats station until end of May) has approximately 5 σ enhancement. It is important to note that only the scintillator with a low energy threshold shows the flux enhancement lasting near 2 h.

Fig. 8 shows disturbances of near-surface electric field measured at Aragats and Nor Amberd research stations. The same lightning was detected at both stations; the distance between the stations is approximately 13 km. Both stations had the same polarity of the electrostatic field (no electrostatic field reversal occurred).

The near-surface electric field at Aragats increased from −43 to 35 kV/min in a very short period; at the Nor Amberd station, the electric field increased from −9 to 23 kV/min. This indicates the occurrence of strong discharge processes nearby in the thunderclouds above Aragats, leading to the decline of the particle flux to the background value, a 14% decrease in 2 s. The start and end of the lightning (time of abrupt enhancing of the near-surface electric field and time of reaching its maximal value) coincide at

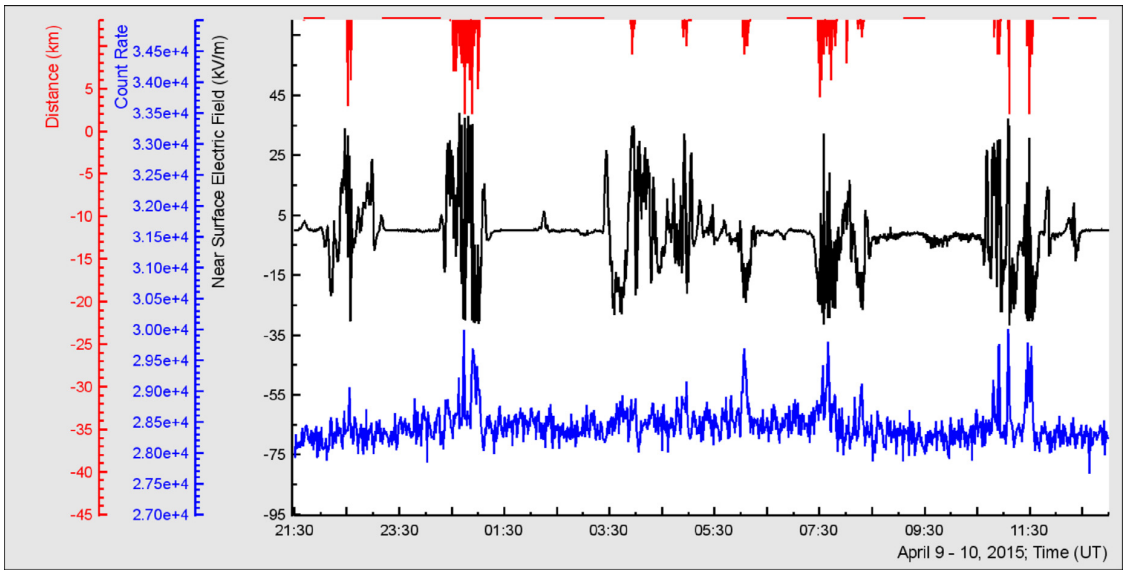

Fig. 9. Time series of particle count rate (bottom); disturbances of near-surface electric field (middle); and distance to lightning (top).

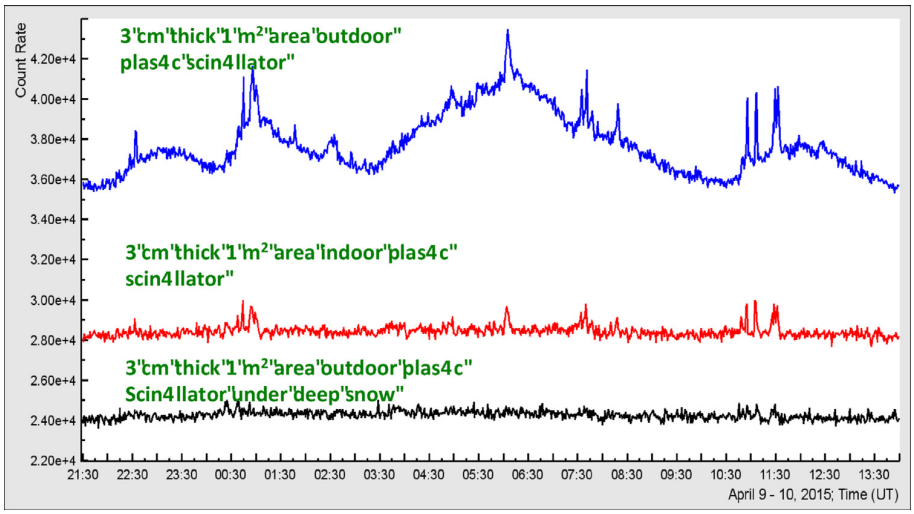

Fig. 10. One-minute time series of the same type of scintillators located under different amounts of matter.

both stations within 50 ms (at 16:00:45.2 and 16:00:45.25 UT), which indicates that the accuracy of synchronization of the remote on-line computers in Nor Amberd and Aragats stations is at least 50 ms. Thus, the measurements of ASEC particle detectors and field-meters are synchronized as well with an accuracy of 50 ms.

4. The long-lasting spring storm of 9–10 April 2015 on Aragats

At 22:00 UT on 9 April 2015, a massive storm hit Mt Aragats. Numerous lightning events occurred near Aragats station for 14 h and the particle flux several times exceeded the background values by 2–22%, which corresponds to 3–32 standard deviations (3–32 σ) in the 1-min time series of the 1-m^2 particle detectors. Humidity was stably high (98%), temperature was near the freezing point ($\sim$−1 °C), and atmospheric pressure was stable as well (684 mbar). The wind traveled from west to north – 160–200°N – at a speed of 5–12 m/s. Fig. 9 shows the 1-min time series of the particle flux measured by the indoor 3-cm-thick, 1-m^2-area plastic scintillator (bottom); the disturbances of electric field measured by EFM-100 electric mill (middle); and estimated distance to the lightning measured by the same electric mill (top). It can be seen from Fig. 9 that almost all disturbances of the electric field were accompanied by lightning events and TGEs.

Fig. 10 also shows the 1-min time series of the same type of particle detectors (3-cm-thick, 1-m^2-area plastic scintillators) located outside, inside, and under deep snow. The weather conditions on high mountains are rather challenging, and the staff cannot maintain some of the outdoor detectors during the winter–spring months. Some of the detectors are operated beneath approximately 1 m of snow; in spring, the snow becomes wet and the particle attenuation in it becomes stronger. It is evident from Fig. 10 that the energy thresholds of all three detectors, despite their similar type, are very different because of the different amount of matter above them. The outside scintillator with the lowest threshold (upper time series) of approximately 1 MeV shows the low-energy component of the TGE lasting up

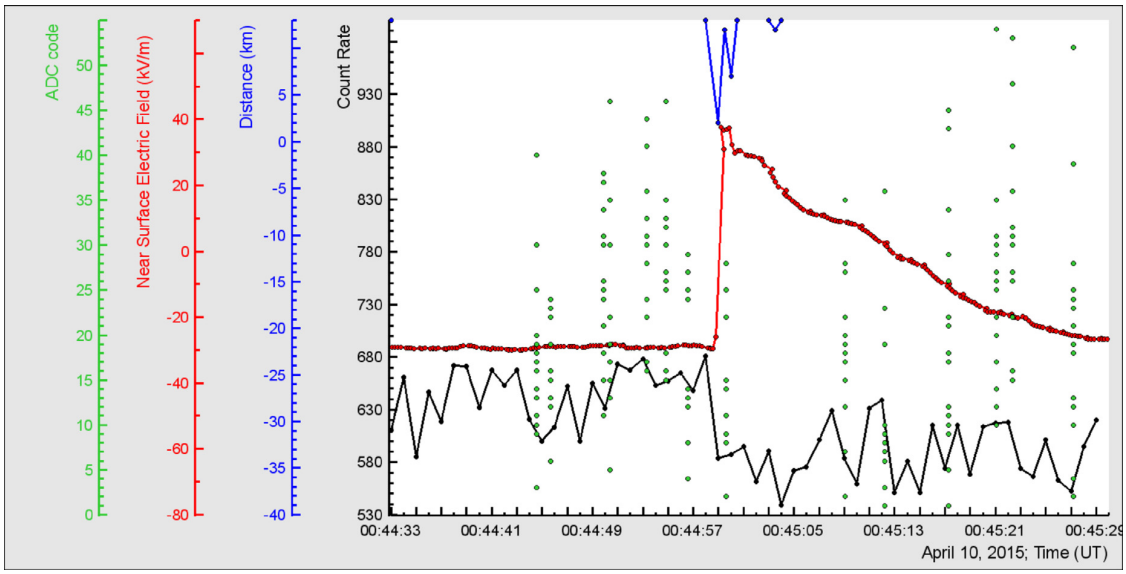

Fig. 11. One-second time series of the count rates measured by the outdoor 3-cm-thick, 1-m^2-area scintillator (bottom); near-surface electric field (middle); distance to lightning (top); and EAS triggers: dots correspond to "fired" ones from 16 plastic scintillators (ADC code is proportional to the number of electrons hitting the scintillator).

to 5 h with emerging peaks of few-minute duration due to RREA bremsstrahlung high-energy gamma photons originated above detector location (measured as well by the scintillators with higher energy threshold seen in the time series in the bottom of the picture 10).

Thus, the scintillators with higher threshold (3–4 MeV) did not register the low-energy component; only peaks from the high-energy gamma rays coincide in time with the ones registered by the low threshold scintillators. From Figs. 9 and 10, we conclude that the low-energy component of TGE is <3–4 MeV. The high-energy component of the TGE is local and is directly related to the RREA process and bremsstrahlung gamma rays; the long-lasting lower energy component of TGE is possibly connected with the distant regions of the thundercloud, where RREA is unleashed and from where Compton-scattered gamma rays reach the detector site.

Fig. 11 shows the data from another TGE terminated by the lightning. From 00:28 to 1:00 UT of April 10, several abrupt surges of the near-surface electric field occurred due to negative lightning events. The near-surface electric field increased from −29 to 40 kV/min in approximately 150 ms at 00:44:58 UT; the electric field recovery time was 29 s. The TGE flux declined by 14% (from 686 to 588) simultaneously with the lightning event and by 21% (down to 541) in the following 4 s.

The time delay between the EAS registered by the scintillators of the MAKET surface array and the start of lightning was 2.25 ± 0.05 s. Thus, we conclude that, for these events, the occurrence of lightning is not related to EAS. According to the RB-EAS theory [19], only very large EASs (with primary energy $>10^{16}$ eV) can facilitate a negative CG lightning; thus, frequent EASs with energies 50–100 TeV cannot be connected with lightning initiation. We need detectors registering cores of very large EASs providing huge ionization in the atmosphere. The small MAKET detector due to fast saturation of scintillators registering EAS electrons cannot outline such events. In general, the core region around the EAS axes is excluded from the recovery of the EAS size and arrival direction. The ArNM and muon detectors, as we will see in the next section by registration of the neutron burst, which are directly connected with the EAS core, can outline the large EAS.

Table 1 summarizes the essential parameters of the selected lightning events that occurred on April 10, 2015. The first column contains the date of the event; the second the time of the abrupt change in the near-surface electric field; the third the time of maximum (for negative lightnings) or minimum (for positive lightnings) and the extreme value of the near-surface electrostatic field; and the fourth the time of the electrostatic field fall or surge. The fifth column contains the drop in the gamma ray flux (if a TGE is released); the sixth the amplitude, that is, the difference between the initial and extreme values of the near-surface electrostatic field; and the seventh the distance to the lightning measured by the EFM-100 electric mill. The last two columns list the coinciding measurements reported by WWLLN (if any).

Of the overall 17 lightning events observed, only three were positive; the positive/negative ratio was approximately 0.18. Abrupt termination of the TGE flux had been observed only during negative lightning events. Positive lightning events show faster dynamics (electric field fall) than the surge of negative lightning events. TGE's surge above background is rather significant $-35 \pm 12\%$. The abrupt decrease of TGE is also sizable $21 \pm 7\%$. From Table 1, we can outline the following typical features of negative CG lightning:

1. Approximate value of mean electric field before the start of the lightning is -24.7 ± 2.9 kV/m
2. The mean maximum value of the enhanced electric field is approximately 51 ± 2.7 kV/m. After reaching maximum, the near-surface electric field slowly returns to pre-lightning values due to continuous charge separation processes in the cloud
3. Mean time from the start of electric field sharp change to its extreme value is approximately 160 ± 50 ms.

The mean distance to lightning is approximately 4.8 ± 3 km. Fig. 12 shows an unusual TGE accompanied with the positive nearby lightning. During a short TGE, the near-surface field was in the positive domain (~37 kV/m), decreasing to 13 kV/m, when the particle flux peaked. The nearby positive lightning (~2 km) at the end of TGE caused the near-surface field to drop from 39 to −31 kV/m.

It is interesting to note that this positive lightning does not terminate the particle flux as the negative ones do.

Table 1
Main parameters of the lightning events occurred on 10 April 2015.

Date (UT)	Start of lightning (UT) and el. field value (kV/m)	Time of maximum (UT) and maximum value (kV/m)	Duration (ms)	Drop of flux (%)	Drop of el. field (kV/m)	Dist. (km)	WWLLN time	WWLLN dist.
10/04/2015	00:38:42.85 8	00:38:43 45	150	–	37	7		
10/04/2015	00:40:45.65 −14	00:40:45:80 36	150	–	50	7		
10/04/2015	00:43:25.65[a] 20	00:4325.90 −42	250	–	−62	7	0:43:25.69	12
10/04/2015	00:44:58.85 −30	00:44:59 40	150	15	70	2		
10/04/2015	00:47:47.7 2	00:47:48.25 22	550	–	20	7		
10/04/2015	00:48:49.10 −4	00:48:49:35 32	250	–	36	3		
10/04/2015	00:51:12.45 1	00:51:12:75 26	300	–	25	7		
10/04/2015	00:53:27.7 −3	00:53:27.9 38	200	–	41	2		
10/04/2015	4:58:06.35 −15	4:58:06.65 8	300	–	23	5		
10/04/2015	7:30:56.4 −23	7:30:56.65 7	250	–	30	4	7:30:56.3	2
10/04/2015	7:32:58.6 −22	7:32:58.9 2	300	–	24	6		
10/04/2015	7:34:35.5 −28	7:34:35:6 36	100	12	64	7		
10/04/2015	7:41:25.05 −24	7:41:25.25 26	200		50	3		
10/04/2015	11:06:39.45[b] 32	11:06:39.5 −32	50	–	−64	2		
10/04/2015	11:26:51.0 −29	11:26:51.2 27	200		56	6		
10/04/2015	11:29:22.15 −27	11:29:22:30 −34	150	10	61	2		
10/04/2015	14:30:11.7[b] 19	14:30:11.75 −30	50	–	−49	14		

[a] Positive lightning was detected in the Nor Amberd station; both electric mills at Aragats registered small negative lightning.
[b] Positive lightning events detected at the Aragats station.

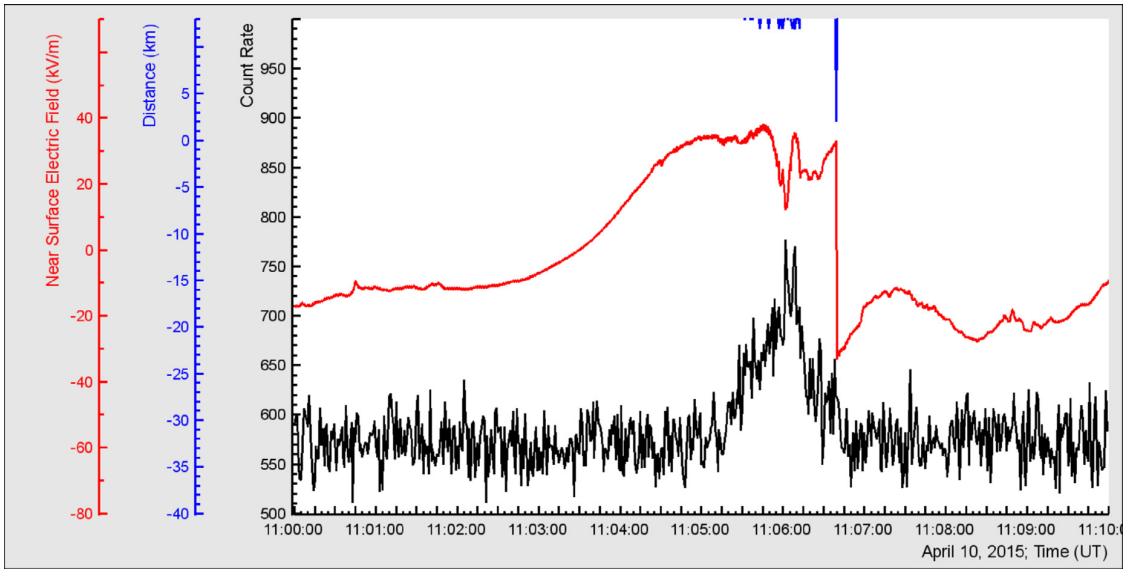

Fig. 12. Rare TGE accompanied by a positive lightning; time series of 1-minute count rate of outdoor 3-cm-thick scintillator (bottom); disturbances of near-surface electric field (middle) and distance to lightning (top).

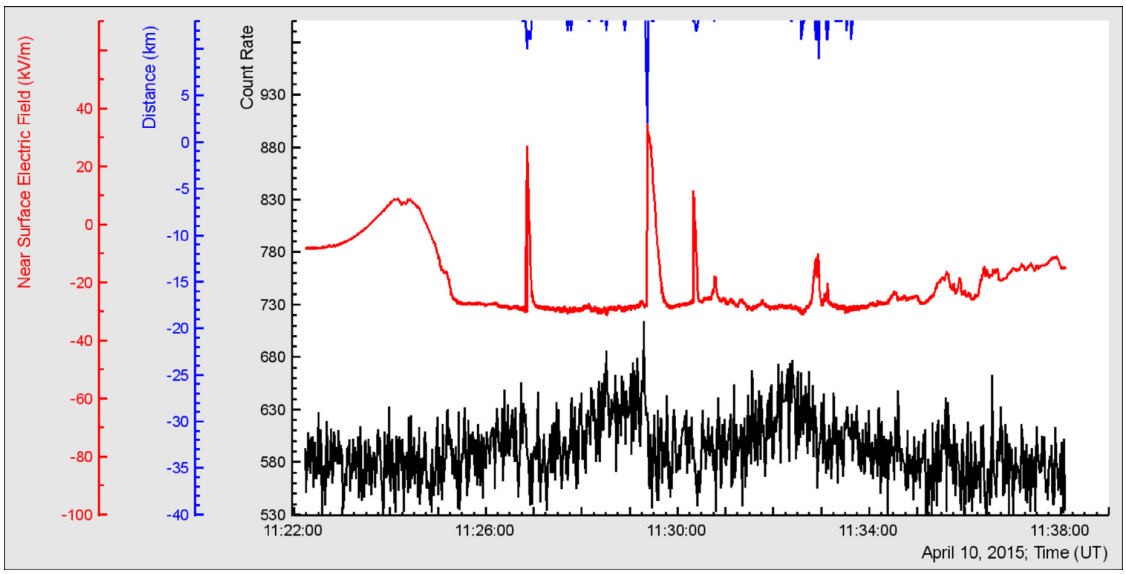

Fig. 13. TGE terminated by four negative lightnings.

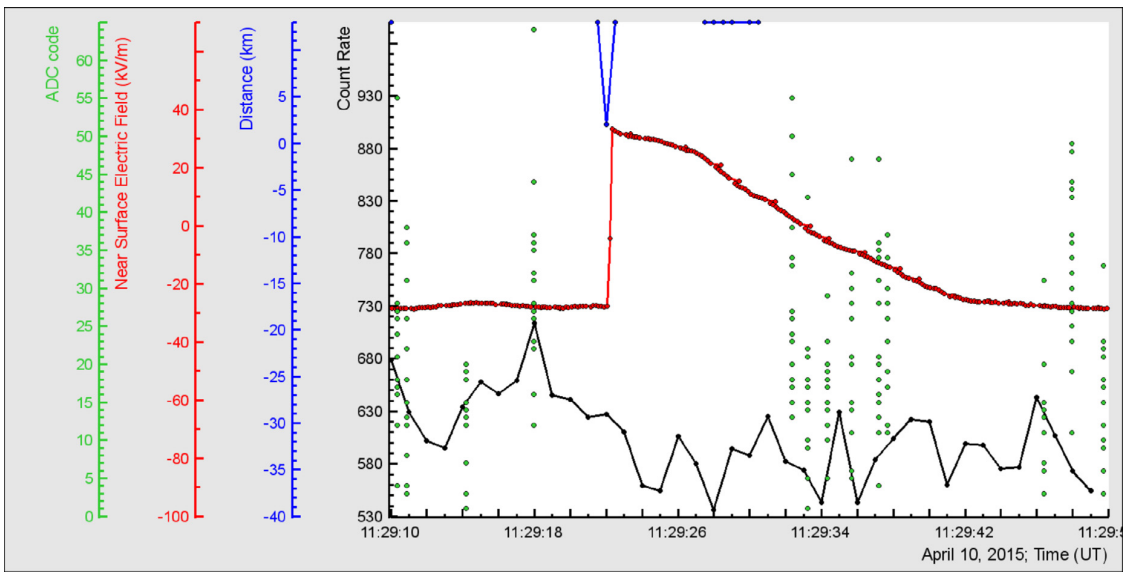

Fig. 14. Zoomed version of Fig. 18. One-second time series of the count rates measured by the outdoor 3-cm-thick, 1-m^2-area scintillator (bottom); near-surface electric field (middle); distance to lightning (top); and EAS triggers: dots correspond to "fired" plastic scintillators (ADC code is proportional to the number of electrons hitting the scintillator).

Fig. 13 shows a TGE several times terminated by the negative lightning. The largest lightning occurred at 11:29:19 UT at < 2 km from the detector site (see zoomed version in Fig. 14); the particle flux dropped by 22% in 4 s. In 200 ms, the near-surface electric field increased from −30 to 27 kV/m, and recovery of the field took 20 s. No coinciding EAS events were detected.

5. Super-event of 20 April 2015

The massive storm of April 19 with many nearby lightning events continued to the next day as well, producing the largest TGE of the last 5 years. At 17:50 UT, the relative humidity of Aragats was very high (~97%); atmospheric pressure was approximately 682 mbar, outside temperature was approximately 2 °C; and velocity of 225°N wind was approximately 3.5 m/s. The electrostatic field was in the negative domain reaching −5 kV/m at 17:50 UT; after two small bumps, the field had near-zero strength after 17:58 UT. The particle count rate increased gradually after 17:58 and rapidly at 17:59, reaching the highest value at 18:00. Fig. 15 shows the time series of 1-min count rate measured by the 1- and 3-cm-thick plastic scintillators, both with area of 1 m^2; the scintillators are located outdoors and have minimum energy thresholds of approximately 1 and 3 MeV. The near-surface electric field with apparent two negative lightning events is shown in the middle of the figure, whereas the top area shows distance to lightning.

The one-minute time series of count rates show huge enhancement comparable with the super-TGEs observed on Aragats in 2009 [6] and 2010 [7]. In 2 min after the TGE start at 17:59 UT, the count rate of the 1-cm-thick scintillator increased from the mean value of 35,540 to 152,430 $(\text{min}*\text{m}^2)^{-1}$, that is to say, the TGE flux

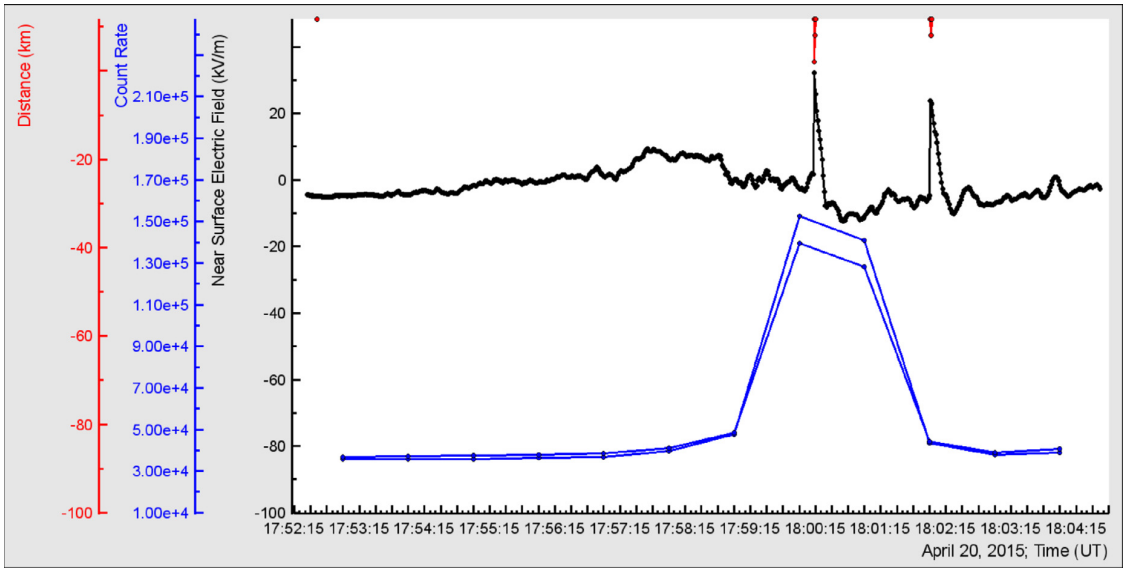

Fig. 15. One-minute count rates of outdoor scintillators (bottom, the larger count rate is corresponding to the 1-cm-thick plastic scintillator with a lower threshold), disturbances of the near-surface electric field (middle), distance to lightning (top), first lightning was observed at a distance of ~2 km and the second one −8 km.

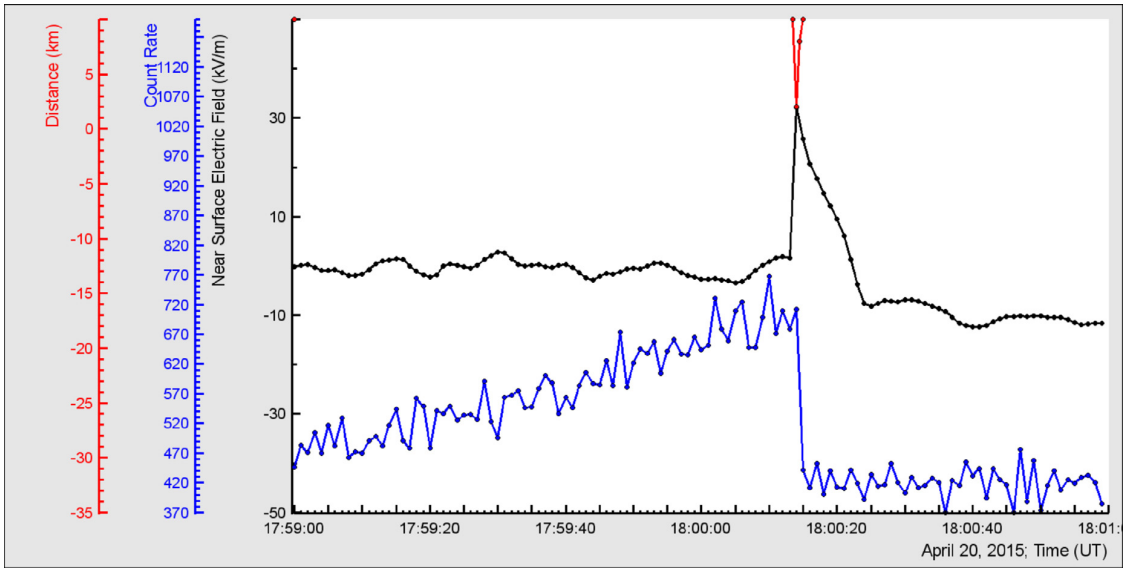

Fig. 16. Immediate decrease of 1-s count rates of the outdoor scintillator (bottom); disturbances of the near-surface electric field (middle); distance to lightning ~2 km (top).

was ~approximately 117,000 $(\text{min}*\text{m}^2)^{-1}$. The flux measured by the 3-cm-thick scintillator was smaller because of higher energy threshold – growing increasing from the mean value of 36,623 to 139,888 $(\text{min}*\text{m}^2)^{-1}$, i.e., approximately 102,000 $(\text{min}*\text{m}^2)^{-1}$. The fluxes were enhanced by 330% and 220%, respectively. The mean square deviation of 1-min count rate of both detectors is approximately 200; therefore, the number of standard deviations ($N\sigma$) is very large – 580 and 500 σ.

The detailed image (1-s time series) of the TGE is shown in Fig. 16, which also shows the 1-s time series of the same 3-cm-thick outdoor plastic scintillator, electric field disturbances, and distances to lightning. The maximal 1-s count rate was observed at 18:00:13 UT. The 3-cm-thick scintillator count rate increased up to 7863 $(\text{s}\,\text{m}^2)^{-1}$; compared with the mean fair weather value of 587 ± 22.6 $(\text{s}\,\text{m}^2)^{-1}$, we obtain 1240% enhancement corresponding to approximately 320 σ; that is, the particle flux was enhanced 12.6 times.

Strong discharge processes within the thunderclouds above Aragats immediately terminate the ongoing huge TGE. The 1-s count rate of 3-cm-thick outdoor scintillator decreases from 7863 $(\text{s}\,\text{m}^2)^{-1}$ at 18:00:13 UT to 5295 (32%) and 598 (92%) at 18:00:14 and 18:00:15 UT, respectively.

A more precise image of the super-TGE event and its possible relationship with an EAS trigger can be seen in the 50-ms time series. Fig. 17 shows the electric field disturbances during the negative lightning observed at Aragats and Nor Amberd stations as well as the 1-s count rates of the 3-cm-thick plastic scintillator. The lightning initiation times registered by the EFM-100 electric mills at the Aragats and Nor Amberd stations were 18:00:14.1 and 18:00:14.15 UT, respectively. The electric field increased from

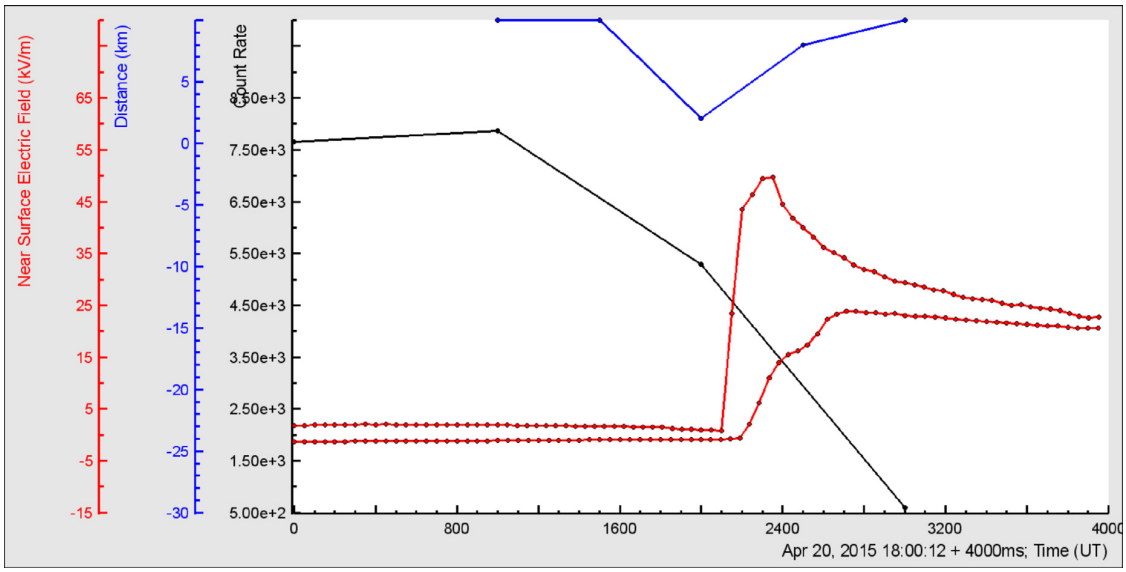

Fig. 17. 50-ms time series of the electric field disturbances during the negative lightning observed at Aragats (rapid increase) and Nor Amberd (gradual increase), and 1-s count rates of 3-cm-thick plastic scintillator.

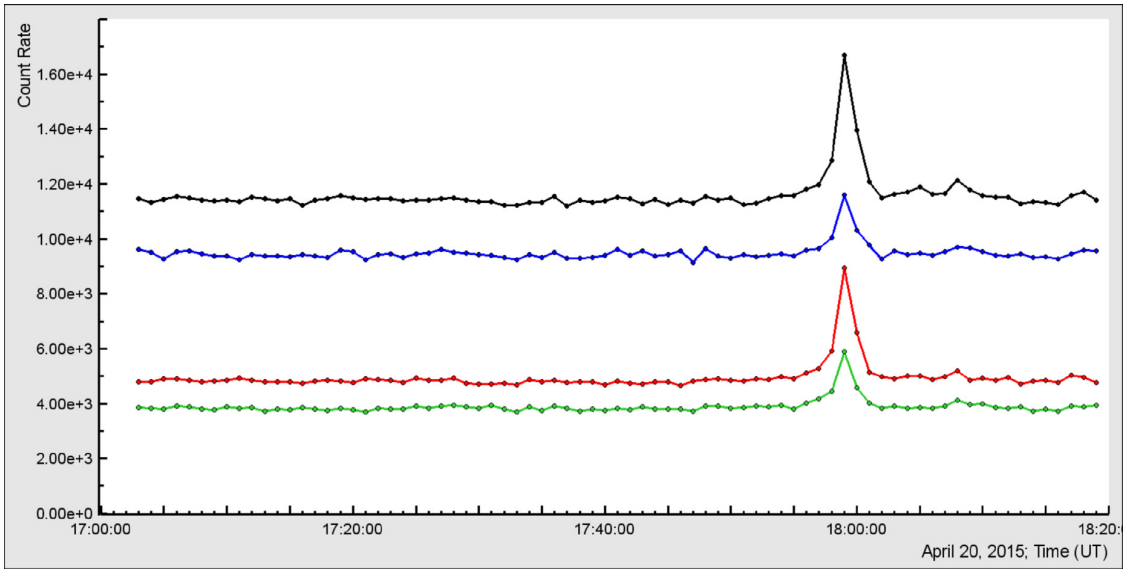

Fig. 18. From top to bottom: count rate of the top 20-cm-thick scintillator without veto; count rate of bottom 20-cm-thick scintillator without veto; count rates with veto switched on.

1.2 to 43.4 kV/m in 100 ms and from 2.15 to 23.8 kV/m in 400 ms at Aragats and Nor Amberd stations, respectively. Field recovering time at Aragats was 10 s (the field decreased to −8 kV/m), and that in Nor Amberd was 30 s. WWLLN registered a strong lightning at 18:00:14.75 UT located 6.7 km away from the Aragats station. The distances to the lightning measured by the EFM-100 sensor from Aragats and Nor Amberd were 1.8 and 5 km, respectively.

By applying the veto system of the Cube detector, we can estimate the fraction of electrons in TGE. Fig. 18 shows the 1-min count rates of two 20-cm-thick plastic scintillators stacked on each other and fully covered by six 1-cm-thick, 1-m^2-area plastic scintillators (for details of CUBE detector, see [13]). The veto signal (at least one hit in six scintillators) from the shielding rejects the charged flux, and it is supposed that only neutral particles reach the inside scintillators and are registered.

However, as the probability of missing charged particles and registration of neural particles is nonzero, corrections need to be made to obtain the electron and gamma-ray fluxes separately.

Using the upper scintillator (with energy threshold equal to ~4 MeV) and applying the techniques described by Chilingarian, Mailyan, and Vanyan [8], we obtain an electron flux intensity of Ie ~ 1000 $(\text{min m}^2)^{-1}$ and gamma-ray flux of Iγ ~ 21,500 $(\text{min m}^2)^{-1}$. For the bottom scintillator of the same type with higher energy threshold, the electron flux was absent and the gamma-ray flux was approximately 2200 $(\text{min m}^2)^{-1}$.

Fig. 19 shows the energy spectrum of the gamma-ray flux measured by a network of NaI spectrometers [10] with an energy threshold of approximately 4 MeV. The electrons with energy in the range of mega-electron volts from the ambient population of the secondary CRs were accelerated in the strong electric fields

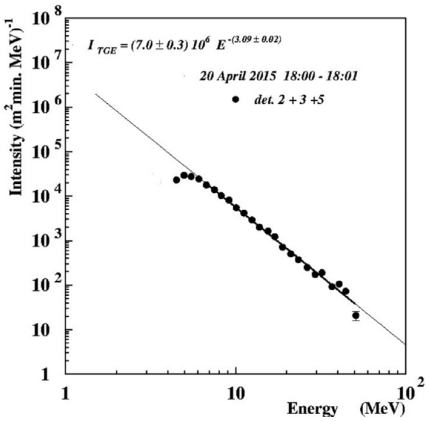

Fig. 19. Differential energy spectrum of the superevent that occurred on 20 April 2015. The spectrometer numbers 2, 3, and 5 involved in the NaI network consisted of five units.

of the thundercloud and runaway, unleashing an electron–photon avalanche. The maximal energy of runaway electrons can be as high as 50 MeV and that of bremsstrahlung gamma rays ranges from 30 to 40 MeV. The very high intensity of TGE indicates that the thundercloud is just above the detector location site. Thus, the bremsstrahlung gamma rays can reach the detector and be registered. Each of the five NaI spectrometers stores a histogram of energy releases every minute. These histograms are added up and a power law fit is applied to the joint histogram.

6. Extensive air showers detected by ArNM and Muon detector

Extensive air showers are initiated by protons or stripped nuclei, which, by interacting with the atmosphere, cause an electron–hadron cascade. Depending on the energy of primary particles, EAS can penetrate the Earth's surface and beneath it (high-energy muons and neutrinos). EAS duration as registered by the surface particle detectors does not exceed a few tens of nanoseconds. However, several detectors containing plenty of absorbing matter can prolong the "life" of EAS to approximately 1 ms. In the neutron monitor's 5-cm lead producer, the EAS hadrons generate several hundreds of neutrons and in the polyethylene moderator they slow the neutrons down to thermal energies before entering the proportional counters. Because of multiple scattering in the absorber and moderator, the time distribution of the secondary neutrons became significantly broader. Thus, the time distribution of the pulses from the proportional counters of the neutron monitor after EAS propagation extends to approximately 1 ms, several orders of magnitude larger than the EAS passing time [3]. The measurements on Tiean-Shan showed that EASs with energy greater than >10 PeV with axes in 3–10 m from NM could produce multiplicities above 1000 [2].

The ArNM (Fig. 3) has a special option for the EAS detection. In general, the dead time of NM is set to approximately 1 ms for one-to-one relation of incident hadrons and detector counts. Thus, neutrons entering the proportional chamber after the first one will be neglected. In ArNM, we use several dead times, and the shortest one, 400 ns, can count almost all the secondary neutrons that enter the proportional chambers. Thus, if ArNM with the shortest dead time registers more signals than with 1-ms dead time, then we conclude that the EAS core hits the detector. Within 1 ms, if we assume very large (continuous) thermalized neutron flux, 2500 thermal neutrons can be registered. It is evident that only extremely energetic EASs hitting NM can produce this very large multiplicity. Fig. 20 shows one of such events with huge total multiplicity of 2310 measured by the shortest dead time of 0.4 μs. The count rate corresponding to larger dead times also enhanced; however, only by 17% (250-μs dead time) and 14% (250 μs dead time). The distribution of multiplicity among eight operational proportional chambers (see inset in Fig. 20) is more or less uniform with the center of gravity of counts in the second section of ArNM (counters 7 and 8).

In Fig. 21, we show another large neutron burst this time detected also by the muon detector. Inset in Fig. 21 shows the enhancement of proportional counters and scintillators of ArNM, muon, and outdoor scintillator without any matter above. The multiplicity (size of the neutron burst) of ArNM is 2060. All three scintillators of muon detector show huge enhancements. The number of coincidences in three scintillators exceeds by an order of magnitude. The outdoor scintillator shows no enhancement at all.

Fig. 22 shows the corresponding enhancements in eight proportional counters of ArNM. The uniform distribution of counts in all sections of ArNM and huge enhancements in muon detector located at a distance of 6 m from ArNM verifies very large size of EAS core, exceeding 10 m. Thus, the energy of the primary particle to initiate EAS was very high.

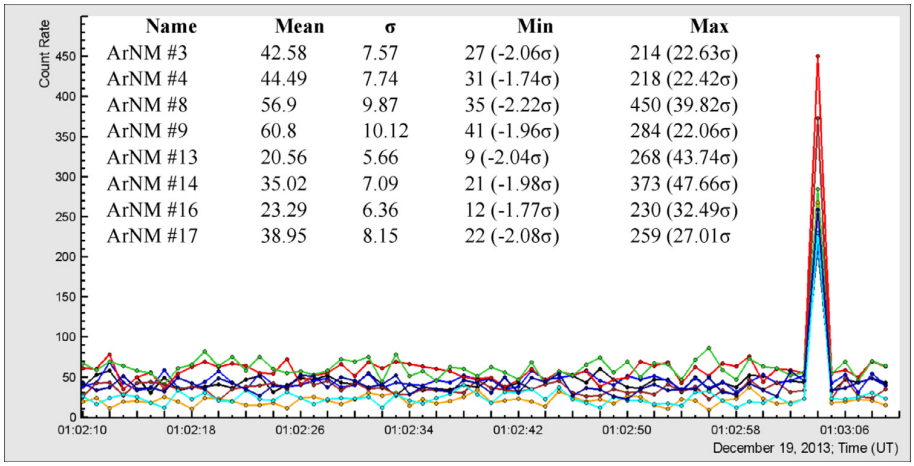

Fig. 20. Time series of ArNM proportional counters registered a large neutron burst at 1:03:4 UT on 19 October 2013. The mean value and variance of the 1-s time series of each counter were calculated by 59 ArNM counts from 1:02:10 to 1:03:9 UT with the second of the neutron burst excluded.

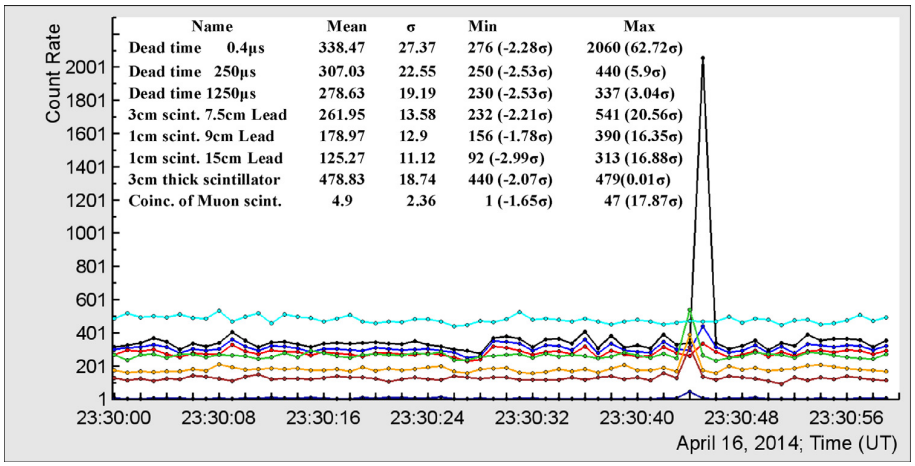

Fig. 21. Large neutron burst detected by the ArNM with dead time of 0.4 μs. All three layers of muon detector and coincidences also show large enhancement (see inset). The 3-cm-thick plastic scintillator shows no enhancement. The 1-s shift in time series of ArNM and muon detectors is explained by the accuracy of time series detected by separate DAQ systems.

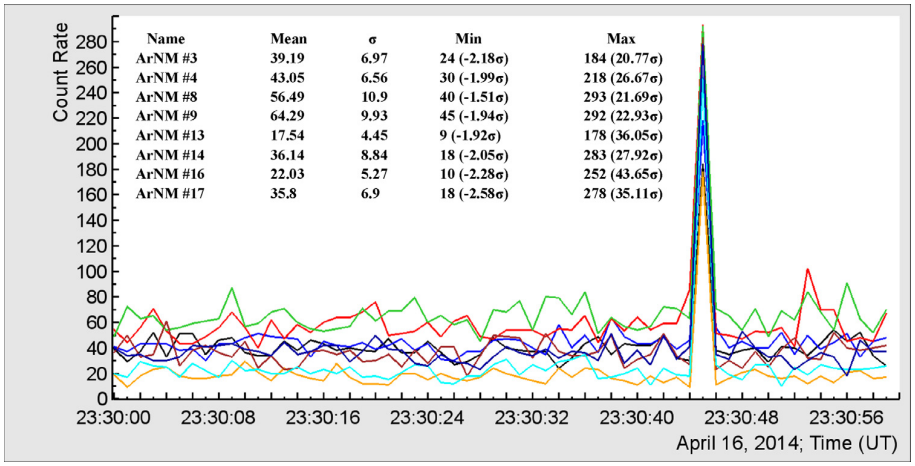

Fig. 22. Time series of ArNM proportional counters registered a large neutron burst at 23:30:45 UT on 16 April 2014. The mean value and variance of the 1-s time series of each counter were calculated by 59 ArNM counts from 23:30 to 23:30:59 UT, by excluding the second of the neutron burst.

Fig. 23 shows the neutron burst multiplicity as a function of the energy of the primary proton-initiated EAS. The relation was obtained by the frequency analysis through the counting intensities of multiplicities (1-s peak counts) of different magnitudes and relating them to the integral energy spectrum measured by the MAKET array at the same place several years ago [4].

The multiplicities above 2000 are extremely rare (one to two per month); neutron bursts detected by both ArNM and muon are even rarer (three to four per year). The primary particle energies corresponding to these events are very high ($>10^{16}$ eV). In the last 3 years, we have detected only two strong negative CG lightning events coinciding with enhancements in muon detector. Unfortunately, at 11:20:53 UT on 19 October 2013, the lightning was so strong that several ASEC particle detectors (including ArNM) remained "blind" for several seconds, including the second of a huge enhancement in muon detector. At 18:00 UT on 20 April 2015, the ArNM was switched off due to electronics failure. Thus, we have two coinciding events of a strong nearby lightning and a very high-energy EAS, which possibly facilitate the propagation of the lightning leader through mature LPCR. These lightning events also immediately terminated a huge TGE on the stage of its maximal flux (Figs. 16 and 17).

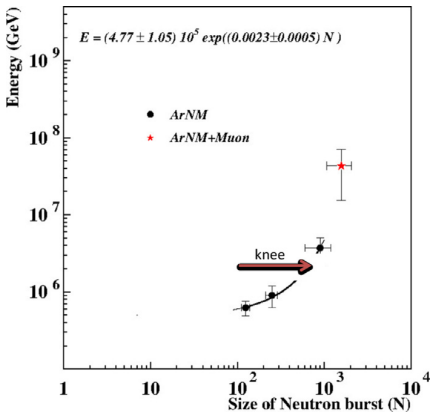

Fig. 23. Dependence of the multiplicity (size) of neutron burst on the energy of the primary particle, which initiated EAS obtained by relation of the frequency of different observed multiplicities (neutron burst sizes) to integral energy spectrum measured by MAKET array [4]. The arrow shows the knee position of the all-particle spectrum and asterisk shows the primary particle energy corresponding to the frequency of detecting bursts both in ArNM and muon detector.

7. Conclusion

April thunderstorms, as usual, also in 2015, make several TGEs observable by ASEC particle detectors and field meters. Using 1-s time series, we have investigated the relationships between lightning and particle fluxes. To the best of the authors' knowledge, this is the first study of its kind to provide vast evidence on simultaneous detection of TGEs, disturbances of the electrostatic field, and lightning. Lightning flashes terminated the particle fluxes very often; during some TGEs, lightning terminated the particle flux thrice. Only a negative lightning can terminate TGEs. No TGE is terminated by a positive lightning. The positive and negative lightning events are classified by the characteristic pattern of disturbance of near-surface electrostatic field, which we measure 20 times per second with a network of EFM-100 electric mills. According to the model [22], lightning terminates particle fluxes mostly in the beginning of TGE or on its decay, when the LPCR is "thinning" and the lightning leader can make a path through it and connect the negatively charge region in the cloud and ground. However, we observed two events (19 October 2013 and 20 April 2015) when huge TGEs were terminated just on the maximum of their development, that is, when LPCR was thick and mature and should prevent the lightning leader to reach the Earth's surface. The muon detector fixed a huge EAS in the same second when the TGE abruptly terminated. Thus, in the same second, we observe sudden termination of TGE at maximal particle flux, a large EAS, and a negative CG lightning. Unfortunately, we do not detect all the three processes on the microsecond time scale. However, following the theory of a combined effect of RB-EAS effect [19], we can assume that the strong ionization in the atmosphere, because of passage of a high-energy EAS ($E > 10^{16}$ eV) under RB conditions, produced a strong local pulse of electric current that initiated a lightning leader and, thereafter, a negative CG lightning. Of course, our findings need to be confirmed by measurements with a microsecond time scale, which are planned for 2016–2017 at Aragats. It is very important to correlate particle flux enhancements and lightning events on millisecond time scales. The lightning is a powerful source of electromagnetic radiation and can affect DAQ electronics and produce fake signals. However, as we showed in Chilingarian et al. [14], the particle flux does not change immediately with a huge pulse of electromagnetic radiation, but with the rearrangement of the electric fields in the cloud after depositing the negative charge to the ground by a lightning. Furthermore, there is a delay of at least several tens of milliseconds between these processes. Therefore, in order to avoid possible interferences and fake signals in the particle detectors, we plan to add a precise time stamp to each registration in the muon detector.

By detecting TGEs with the same type of detectors, although different amount of matter above and, therefore, having different energy thresholds, we prove the existence of two components of particle population in the TGE. The high-energy one (from 3–4 to 40–50 MeV) is local and of short duration (several minutes) and is related to the RB/RREA process above the detectors, resulting in bremsstrahlung gamma photons. The second, low-energy component (0.4–3 MeV) lasted several hours and, as we admit, is associated with the Compton-scattered gamma rays that reach the detectors from the distant regions of the cloud.

Acknowledgments

The authors thank the staff of the Aragats Space Environmental Center for the uninterruptible operation of Aragats research station facilities. The data for this study were made available by the multivariate visualization software ADEI on the WEB page of the Cosmic Ray Division (CRD) of the Yerevan Physics Institute, http://adei.crd.yerphi.am/adei. The authors wish to thank the World Wide Lightning Location Network (http://wwlln.net), collaboration among more than 50 universities and institutions, for providing the lightning location data used in this study. The expedition to Aragats high-altitude station was supported by the Armenian Government Grant N13-1C275.

References

[1] V.V. Alexeenko, N.S. Khaerdinov, A.S. Lidvansky, V.B. Petkov, Transient variations of secondary cosmic rays due to atmospheric electric field and evidence for pre-lightning particle acceleration, Phys. Lett. A 301 (2002) 299–306.
[2] A.P. Antonova, A.P. Chubenko, S.V. Kruychkov, et al., Anomalous time structure of extensive air shower particle flows in the knee region of primary cosmic ray spectrum, J. Phys. G: Nucl. Part. Phys. 28 (2002) 251–266.
[3] Yu.V. Balabin, B.B. Gvozdevsky, E.V. Vashenyuk, D.D. Dzhappuev, EAS hadronic component as registered by a neutron monitor, Astrophys. Space Sci. Trans. 7 (2011) 507–510.
[4] A. Chilingarian, G. Gharagyozyan, G. Hovsepyan, S. Ghazaryan, L. Melkumyan, A. Vardanyan, Light and heavy cosmic-ray mass group energy spectra as measured by the MAKET-ANI detector, Astrophys. J. 603 (2004) L29–L32.
[5] A. Chilingarian, K. Arakelyan, K. Avakyan, et al., Correlated measurements of secondary cosmic ray fluxes by the Aragats Space-Environmental Center monitors, Nucl. Instrum. Methods Phys. Res. Sect. A 543 (2–3) (2005) 483–496.
[6] A. Chilingarian, A. Daryan, K. Arakelyan, et al., Ground-based observations of thunderstorm-correlated fluxes of high-energy electrons, gamma rays, and neutrons, Phys. Rev. D 82 (2010) 043009.
[7] A. Chilingarian, G. Hovsepyan, A. Hovhannisyan, Particle bursts from thunderclouds: natural particle accelerators above our heads, Phys. Rev. D 83 (2011) 062001.
[8] A. Chilingarian, B. Mailyan, L. Vanyan, Recovering of the energy spectra of electrons and gamma rays coming from the thunderclouds, Atmos. Res. 114–115 (2012) 1–16.
[9] A. Chilingarian, H. Mkrtchyan, Role of the lower positive charge region (LPCR) in initiation of the thunderstorm ground enhancements (TGEs), Phys. Rev. D: Part. Fields 86 (2012) 072003.
[10] A. Chilingarian, G. Hovsepyan, L. Kozliner, Thunderstorm ground enhancements: gamma ray differential energy spectra, Phys. Rev. D 88 (2013) 073001.
[11] A. Chilingarian, Thunderstorm Ground Enhancements – model and relation to lightning flashes, J. Atmos. Solar-Terr. Phys. 107 (2014) 68–76.
[12] A. Chilingarian, S. Chilingaryan, G. Hovsepyan, Calibration of particle detectors for secondary cosmic rays using gamma-ray beams from thunderclouds, Astropart. Phys. 69 (2015) 37–43.
[13] A. Chilingarian, G. Hovsepyan, G. Khanikyanc, A. Reymers, S. Soghomonyan, Lightning origination and thunderstorm ground enhancements terminated by the lightning flash, EPL 110 (2015) 49001.
[14] A. Chilingarian, G. Hovsepyan, Y. Khanikyants, D. Pokhsraryan, S. Soghomonyan, Atmospherics discharges – particle flux relations in the TGEs terminated by the lightning flash, in: Proceedings of TEPA 2015, Nor Amberd , Tigran Metz, 2016.
[15] J.R. Dwyer, D.M. Smith, S.A. Cummer, High-energy atmospheric physics: terrestrial gamma-ray flashes and related phenomena, Space Sci. Rev. 173 (2012) 133–196.
[16] J.R. Dwyer, M.A. Uman, The physics of lightning, Phys. Rep. 534 (4) (2013) 147–241.
[17] G.J. Fishman, P.N. Bhat, R. Mallozzi, J.M. Horack, T. Koshut, C. Kouveliotou, G.N. Pendleton, C.A. Meegan, R.B. Wilson, W.S. Paciesas, S.J. Goodman, H.J. Christian, Discovery of intense gamma ray flashes of atmospheric origin, Science 264 (5163) (1994) 1313–1316.
[18] A.V. Gurevich, G.M. Milikh, R Rouseel-Dupre, Runaway electron mechanism of air breakdown and preconditioning during a thunderstorm, Phys. Lett. A 1992 V.165 (1992) 463–468.
[19] A.V. Gurevich, K.P Zybin, R.A. Roussel-Dupre, Lightning initiation by simultaneous of runaway breakdown and cosmic ray showers, Phys. Lett. A 254 (1999) 79.
[20] N.A. Kelley, D.M. Smith, J.R. Dwyer, et al., Relativistic electron avalanches as a thunderstorm discharge competing with lightning, Nat. Commun. 6 (2015) Article no: 7845.
[21] P. Krehbeil, V. Mazur, W. Rison, Standardizing the sign convention for atmospheric electric field measurements, Newslett. Atmos. Electr. 5 (2) (2014) 5.
[22] A. Nag, V.A. Rakov, Some inferences on the role of lower positive charge region in facilitating different types of lightning, Geophys. Res. Lett 36 (2009) L05815.
[23] Yu.V. Stenkin, D.D. Djappuev, J.F. Valdés-Galicia, Neutrons in extensive air showers, Phys. At. Nucl. 70 (2007) 1088–1099.
[24] H. Tsuchiya, T. Enoto, K. Iwata, et al., Detection of high-energy gamma rays from winter thunderclouds, Phys. Rev. Lett. 111 (2013) 015001.
[25] M Stolzenburg, W Rust, T Marshall, Electrical structure in thunderstorm convective regions 3. Synthesis, J. Geophys. Res. 103 (1998) 14097–14108.